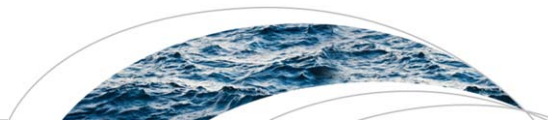


Correcting artifacts in transition to a wound optic fiber: Example from high-resolution temperature profiling in the Dead Sea

The Faculty of Oregon State University has made this article openly available.
Please share how this access benefits you. Your story matters.

Citation	Arnon, A., J. Selker, and N. Lensky (2014). Correcting artifacts in transition to a wound optic fiber: Example from high-resolution temperature profiling in the Dead Sea. <i>Water Resources Research</i> , 50(6), 5329–5333. doi:10.1002/2013WR014910
DOI	10.1002/2013WR014910
Publisher	American Geophysical Union
Version	Version of Record
Terms of Use	http://cdss.library.oregonstate.edu/sa-termsfuse



TECHNICAL NOTE

10.1002/2013WR014910

Key Points:

- Structured artifacts at the transition to a high-resolution helically wound optic fiber
- Correction of the artifact is suggested here

Correspondence to:

N. Lensky,
nadavl@gsi.gov.il

Citation:

Arnon, A., J. Selker, and N. Lensky (2014), Correcting artifacts in transition to a wound optic fiber: Example from high-resolution temperature profiling in the Dead Sea, *Water Resour. Res.*, 50, 5329–5333, doi:10.1002/2013WR014910.

Received 16 OCT 2013

Accepted 27 MAY 2014

Accepted article online 2 JUN 2014

Published online 27 JUN 2014

Correcting artifacts in transition to a wound optic fiber: Example from high-resolution temperature profiling in the Dead Sea

Ali Arnon^{1,2}, John Selker³, and Nadav Lensky¹

¹Geological Survey of Israel, Jerusalem, Israel, ²Department of Geology and Environment, Bar Ilan University, Ramat Gan, Israel, ³Department of Biological & Ecological Engineering, Oregon State University, Corvallis, Oregon, USA

Abstract Spatial resolution fiber-optic cables allow for detailed observation of thermally complex heterogeneous hydrologic systems. A commercially produced high spatial resolution helically wound optic fiber sensing cable is employed in the Dead Sea, in order to study the dynamics of thermal stratification of the hypersaline lake. Structured spatial artifacts were found in the data from the first 10 m of cable (110 m of fiber length) following the transition from straight fiber optic. The Stokes and Anti-Stokes signals indicate that this is the result of differential attenuation, thought to be due to cladding losses. Though the overall spatial form of the loss was consistent, the fine structure of the loss changed significantly in time, and was strongly asymmetrical, and thus was not amenable to standard calibration methods. Employing the fact that the cable was built with a duplex construction, and using high-precision sensors mounted along the cable, it was possible to correct the artifact in space and time, while retaining the high-quality of data obtained in the early part of the cable (prior to significant optical attenuation). The defect could easily be overlooked; however, reanalyzing earlier experiments, we have observed the same issue with installations employing similar cables in Oregon and France, so with this note we both alert the community to this persistent concern and provide an approach to correct the data in case of similar problems.

1. Background

High-resolution temperature profiling of the thermally stratified Dead Sea was conducted using high-resolution (HR) helically wound fiber-optic profiler, aiming to explore the dynamics of thermal stratification of the hypersaline lake [Arnon *et al.*, 2014]. An artifact in the temperature profiling was found, it is an inherent artifact in the used HR profilers. The aim of this paper is to help identifying this artifact and to propose a correction procedure, to enable accurate temperature sensing along the entire profiler.

2. The Observation System Setup

The observation system setup is presented in Figure 1. A profiler, 55 m vertically oriented, duplex HR optic fiber (BRUsens 70°C high-resolution, Brugg Cables, Brugg Switzerland) was suspended from a buoy; the HR cable was connected to a duplex 0.01 m diameter marine cable (BRUsens Submarine, Brugg Cables, Brugg, Switzerland) running to the shore along the bottom of the Sea (Figure 1). Both cables were produced using Corning (Corning, New York) ClearCurve bend-optimized fiber, and terminated with E2000 APC connectors, joined by barrel connectors. The cable employs a duplex version of the “wrapped pole” method described by Selker *et al.* [2006] to achieve the enhanced vertical resolution: two fibers were helically wound around a 0.020 m core, with each fiber contained in a 0.0023 m OD plastic tube. With a 0.002 m polyurethane jacket, this yielded a cable with a 0.026 m OD, wherein each 0.09 m of cable length represented 1 m of optical path, which is the spatial sampling of the instrument (DTS). The two fibers of the HR cable were fusion spliced at the far end to make a single optical path. The marine cable was connected at the shore to a Distributed Temperature Sensing instrument (DTS, Sensornet Oryx+, Hertfordshire, UK). Both cables were operated in duplex mode with the light traveling from the shore to the sea to the bottom of the HR cable and (continuously) coming back to the buoy and back to the DTS on shore. The calibration of the vertical cable (presented hereafter) made use of two high-precision data logging thermistors (Sea Bird SBE39) attached at depths of 10 and 50 m along the HR cable (Figure 1).

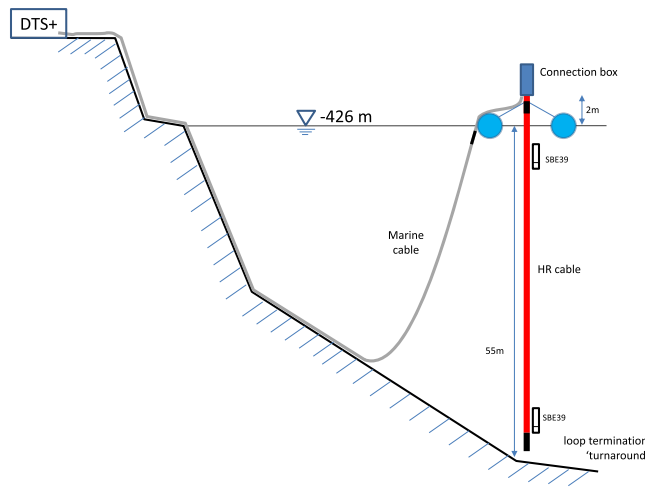


Figure 1. A schematic illustration of the fiber-optic measurement system in the Dead Sea. The gray line indicates the path of the 0.010 m diameter marine cable, and the red line the HR cable. The buoy (with floats indicated by the blue circles) was held in place by four cables tied to 400 kg concrete blocks (not shown). A 20 kg steel weight (shown as the black section at the lowest point on the HR cable) maintained constant vertical orientation.

3. Stokes Signal— Unexpected Gradual Decrease

The Stokes signal, which is largely temperature independent, showed an unexpected gradual decay along the fiber as it entered the wound cable following the connector, quite distinct from a typical “step” drop of signal due to loss of light sometimes seen at connectors (not evident here; Figure 2) [see discussion in Tyler *et al.*, 2009]. The signal decay spans about 100 m of fiber (thus, about 10 m of vertical path of the HR cable in the Sea). Unlike most differential attenuation in fiber-optic cables, this loss is asymmetrical, depending on the direction of light travel, attenuating light immediately following insertion of light into the HR cable, but absent

when the light travels along the same fiber when the light is injected in the alternate end of the cable as is carried out with double-ended measurements (see the two boxes in Figure 2 on the entrance to and the exit from the HR cable).

With Raman DTS, temperature along the fiber is calculated from the ratio of the Stokes and anti-Stokes signal, typically requiring three calibration values specific to the cable and instrument [e.g., Hausner *et al.*, 2011; van de Giesen *et al.*, 2012]. Because the HR cable was duplexed, at each location along the profiler there were two readings, one from the signals traveling on the fiber which leads away from the instrument (“outgoing”), and the second parallel fiber which is physically fused to the first leading back to the

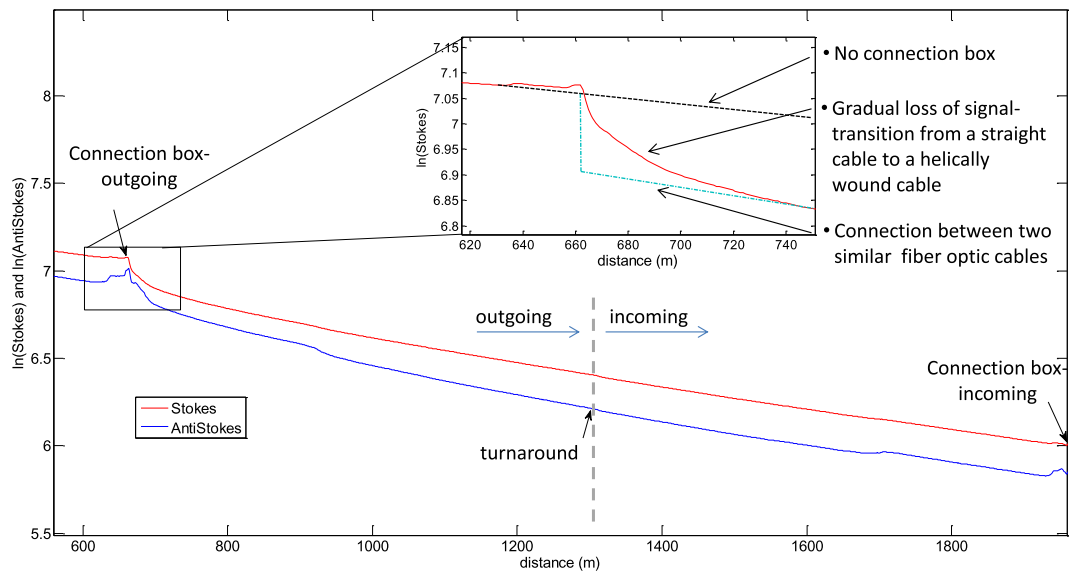


Figure 2. Stokes and anti-Stokes signals along the HR cable (starting at 565 m). Distance is indicated in meters of fiber optic from the DTS. Insert focuses in the connection box area where the light enters the HR cable, showing that the decay was not typical of isolated step losses of light associated with connections between fibers. Notice that the Stokes signal does not show a similar decay on the incoming signal of the HR cable (compare the two arrows). The rise in the anti-Stokes signal prior to the connection to the HR cable reflects the transition in temperature from the floor of the Dead Sea to the buoy, and the local high temperature at the connection box which is in the air.

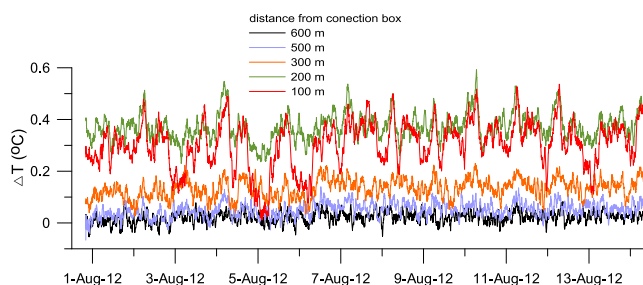


Figure 3. Ten day time series of calculated apparent temperature difference (discrepancy) between computed temperature values from light traveling down and up the HR cable at 100 m increments; temperatures computed using a constant differential attenuation per cable length. Distances reported are along the HR cable from the connection box (100 m along the cable is physically ~11 m of profiler). The fine-scale variability of the plotted data illustrates the fundamental noise of the data, which employed a 5 min integration time (about 0.05°C). The diminishing offsets between data taken at successively greater distances from the connection box illustrate the diminishing impact of the asymmetrical loss with distance from the connector.

accuracy, since both readings reflect the same temperatures. The observed discrepancy in computed temperature between outgoing and incoming light is dramatically greater near the connection box (100 and 200 m from the connection box) relative to the rest of the profiler (300–600 m; Figure 3). Further, the apparent temperature difference is strongly time dependent, seemingly related to the diurnal and other temperature changes. Though the mechanism of this light loss is not certain, it is consistent with differential attenuation due to microbending losses which we believe to be the basis of the spatial loss of light responsible for the overall artifact, which may be accentuated or diminished as the cable expands and contracts with changes in temperature.

We hypothesize that the light is experiencing a gradual loss of the most extreme modes of light in the multimode fiber due to the transition to a curving optic fiber. Those modes, which are striking the index of refraction break in the fiber at near the acceptance angle of the fiber, will see slightly greater interface angles due to the bending of the fiber. While both Stokes and anti-Stokes wavelengths may experience such loss, since the angle of acceptance is different for the two frequencies, they lose different fractions of the total intensity. This loss mechanism would be expected to follow a Beer’s law pattern, explaining the approximately exponential shape to the data seen in Figure 2, and evidenced in the computed temperature anomalies of Figure 3 where the loss rate clearly diminishes away from the injection of light into the HR cable. Under this hypothesis, one might expect that the defect would be constant in time, and could be corrected by the addition of a directional spatially distributed differential attenuation term in the HR cable. Clearly this is not the case. Further, the usual assumptions of symmetry in optical loss required for use of either duplex or double-ended methods of correction for differential attenuation are rendered inapplicable [van de Giesen et al., 2012].

4. Correcting for Directional Differential Attenuation

Due to the violation of symmetry and time-independence required for analytical strategies, we chose to handle the correction empirically. Recognizing that the light loss extends about 100 m along the fiber (only 1/5th of the depth of the profiler), the simplest solution is to ignore the data from immediately after the connection, and to compute the temperatures in this area using only the incoming signal. In this approach, the “defective” data found in the fiber immediately after the insertion of light in the HR cable are discarded, and a full temperature profile is achieved without specifically addressing the “entrance effect.” The disadvantage in this approach is the loss of the higher-quality signal, since the light levels are substantially lower in the HR on the incoming compared to the outgoing fibers (Figure 2—note the logarithmic scale on the vertical axis).

Because the pattern of loss changed relatively slowly in both space and time, we were able to compute a moving-average correction per depth that did not add significant noise to the data: as discussed below, the corrections were computed as averages of 120 data points in space and time, thus the statistical noise on

instrument (“incoming”) at the fiber “turnaround.” The outgoing fiber sends light down the profiler. After the turnaround, this light arrives at each location along the cable in reverse order along the incoming fiber (for instance, the incoming light traveled up the profiler). The DTS could have been programmed to alternate on which fiber the light was launched, which is referred to as “Double-ended” operation. This was not done here, rather employing the duplex single-ended approach [see van de Giesen et al., 2012]. The calculated temperature along these parallel sections provides a quality control on the measured temperature accu-

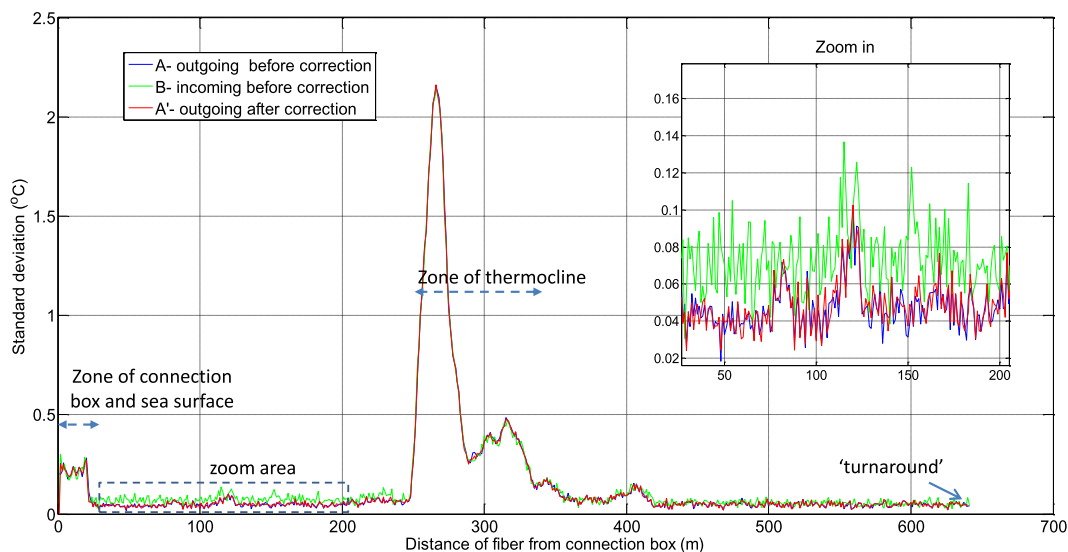


Figure 4. Temperature STD of every node on the fiber based on a moving window of 10 sequential readings. In blue—the outgoing (A), in green—the incoming (B), and in red—the outgoing after correction (A').

these data were an order of magnitude less than the noise on the individual measurements, and so the correction did not add statistical uncertainty to the data. In general, this correction could be made in simplex cables where such a returning signal would not be available so long as sufficient calibration data were available, though the duplex cable is highly advantageous since it provides hundreds of points at which temperatures can be compared. To compute the spatial correction with minimal impact of reading noise, we employed a spatial and temporal moving average of 10 m of fiber and 1 h (i.e., averaging 120 measurements taken at 1 m and 5 min), respectively, on the temperatures obtained from the outgoing (B), and incoming (A) fibers each meter along the fibers and at each time. The incoming temperatures were known to be correct in the mean, having well calibrated to the external sensors, and showing precisely the expected behaviors of constant spatial temperature distribution across zones, which would be expected to be well mixed from a fluid-mechanical analysis. Though these returning data are noisier due to attenuation of light with distance along the cable, this noise was effectively eliminated from the correction by taking sufficient averaging in time-space (since the noise drops with the square root of the number of samples which are averaged, here $120^{1/2}$, which is thus about 11 times lower noise). It was fortunate that there was such a scale separation between the defect and the instrument resolution. The difference between these time-space averaged computed temperatures was added to the temperatures of the outgoing section as expressed in equation (1).

$$A' = A + (\langle B \rangle - \langle A \rangle) \tag{1}$$

Angled brackets signify temporal and spatial averaging, and A' is the corrected outgoing signal.

Figure 4 presents the standard deviation (STD) of each DTS reported temperature node. The STD was computed based on reported measurements from 10 sequential time steps, on the outgoing signal before correction (A), after correction (A'), and on the incoming (B). The greatest differences in the STD values along the cable are associated with large shifts in environmental conditions (temperature) in specific sections along the cable (e.g., the thermocline at 250–350 m of fiber which is ~25 m deep in the water and the area of the connection box at 0–30 m of fiber). Nevertheless, there is a gradual increase in STD values along the fiber due to the decreasing signal to noise ratio along the light's travel path. As expected, it can be seen that the outgoing A' section benefits from smaller STD than the incoming B section. Thus this correction maintains fidelity to the mean temperature obtained from the upward measurements, but keeps the greater signal to noise obtained from the outward traveling light which has greater intensity, and therefore lower random noise.

5. Summary

Without correction beyond standard calibration the HR cable employed had temperature anomalies of magnitude of up to 0.5°C. Though not earlier recognized, such asymmetrical losses have since been detected using similar helically wound cables, as well in river installations where straight cables made abrupt corners (data not shown). This leads us to believe that this issue may well be relevant in many applications of DTS in environmental monitoring. These Dead Sea anomalies may be close to the worst case, arising from continuously bent fiber in plastic housings that deformed with temperature. This led the asymmetrical losses to be strongly time and space dependent, and therefore not amenable to standard calibration strategies. Because the defect was only seen in the first 100 m of optical path, it allowed for correction based on the dual measurements obtained from the duplex cable, wherein the true temperature was computed from the light that had traversed enough of the cable for this loss mechanism to have been completed. The procedure presented here, based on comparison to reference temperatures and duplex measurements, provided temperature data accurate to 0.05°C each 5 min, which is as good as could have been obtained from normal cables for the DTS used to obtain these data, thus eliminating the errors due to the asymmetrical loss without appreciable loss of resolution.

Acknowledgments

We thank the Taglit R/V team: Silvi Gonen, Meir Yifrach, and Shachar Gan-El for their construction of the buoy and its maintenance, Isaac Gertman and Tal Ozer for their assistance and guidance of the buoy construction, Ittai Gavrieli, Raanan Bodzin, and Hallel Lutsky for their assistance and discussions, and Thomas Hertig for discussions and the designing of the optical cables. Selker thanks the NSF for support of his time through the Center for Transformative Environmental Monitoring Programs (CTEMPs), and the Geological Survey of Israel for support of his travel expenses.

References

- Arnon, A., N. Lensky, and J. S. Selker (2014), High-resolution temperature sensing in the Dead Sea using fiber optics, *Water Resour. Res.*, *50*, 1756–1772, doi:10.1002/2013WR014935.
- Hausner, B. M., F. Suárez, E. K. Glander, N. van de Giesen, J. S. Selker, and S. W. Tyler (2011), Calibrating single-ended fiber-optic Raman spectra distributed temperature sensing data, *Sensors*, *11*, 10859–10879, doi:10.3390/s111110859.
- Selker, J. S., L. Thévanaz, H. Huwald, A. Mallet, W. Luxemburg, N. van de Giesen, M. Stejskal, J. Zeman, M. C. Westhoff, and M. B. Parlange (2006), Distributed fiber-optic temperature sensing for hydrologic systems, *Water Resour. Res.*, *42*, W12202, doi:10.1029/2006WR005326.
- van de Giesen, N., C. Susan, S. Dunne, J. Jansen, O. Hoes, M. B. Hausner, S. Tyler, and J. Selker (2012), Double-ended calibration of fiber-optic Raman spectra distributed temperature sensing data, *Sensors*, *12*, 5471–5485, doi:10.3390/s120505471.